Mat. Res. Soc. Symp. Proc. Vol. 765 © 2003 Materials Research Society

Investigation and modeling of fluorine co-implantation effects on dopant redistribution

M. Diebel[1,2], S. Chakravarthi[2], S.T. Dunham[3], C.F. Machala[2], S. Ekbote[2], A. Jain[2]
[1]Department of Physics, Univ. of Washington, Seattle, WA 98195-1560, USA
[2]Silicon Technology Development, Texas Instruments, Dallas, TX 75243, USA
[3]Department of Electrical Engineering, Univ. of Washington, Seattle, WA 98195-2500, USA

ABSTRACT

A comprehensive model is developed from *ab-initio* calculations to understand the effects of co-implanted fluorine (F) on boron (B) and phosphorus (P) under sub-amorphizing and amorphizing conditions. The depth of the amorphous-crystalline interface and the implant depth of F are the key parameters to understand the interactions. Under sub-amorphizing conditions, B and P diffusion are enhanced, in contrast to amorphized regions where the model predicts retarded diffusion. This analysis predicts the F effect on B and P to be entirely due to interactions of F with point-defects.

INTRODUCTION

As ULSI devices enter the nanoscale, ultra-shallow junctions become necessary. Reduction in transient enhanced diffusion (TED) and enhanced dopant activation are desired. Experimentally, co-implanted F has been shown to reduce B and P TED [2, 3, 4, 5, 6] as well as enhance B activation [2, 3]. However, to utilize these benefits effectively, a fundamental understanding of the F behavior is necessary, particularly since implanted F has been observed to behave unusually in silicon, manifesting an apparent uphill diffusion [1]. Also we find that depending on the implant conditions F can actually enhance B diffusion (see Fig. 4 (right)). This paper focuses on the effects of co-implanted F on dopant redistribution. Previously reported *ab-initio* calculation results [7] were used to develop a comprehensive model to analyze and explain the effects of co-implanted F on B and P redistribution under various implant conditions.

MODEL

Theoretically, F can affect B and P diffusion in at least two distinct ways. A direct interaction could explain the reported F effects if there is a large binding energy between dopant and F atoms. The second possibility is an indirect interaction. If F interacts strongly with point-defects, it alters the local point-defect concentrations, changing the point-defect mediated diffusion behavior of B and P. *Ab-initio* calculations find only about 1eV binding for dopant-fluorine complexes (B-F and P-F), which is insufficient to significantly influence diffusion behavior [8]. In contrast, strongly bound fluorine vacancy clusters (F_nV_m) were identified [7]. This suggests that the effects of F on B and P are primarily due to fluorine point-defect interactions. In this case, it is expected that once the anomalous F diffusion is understood, the same model should also explain the effects on B and P.

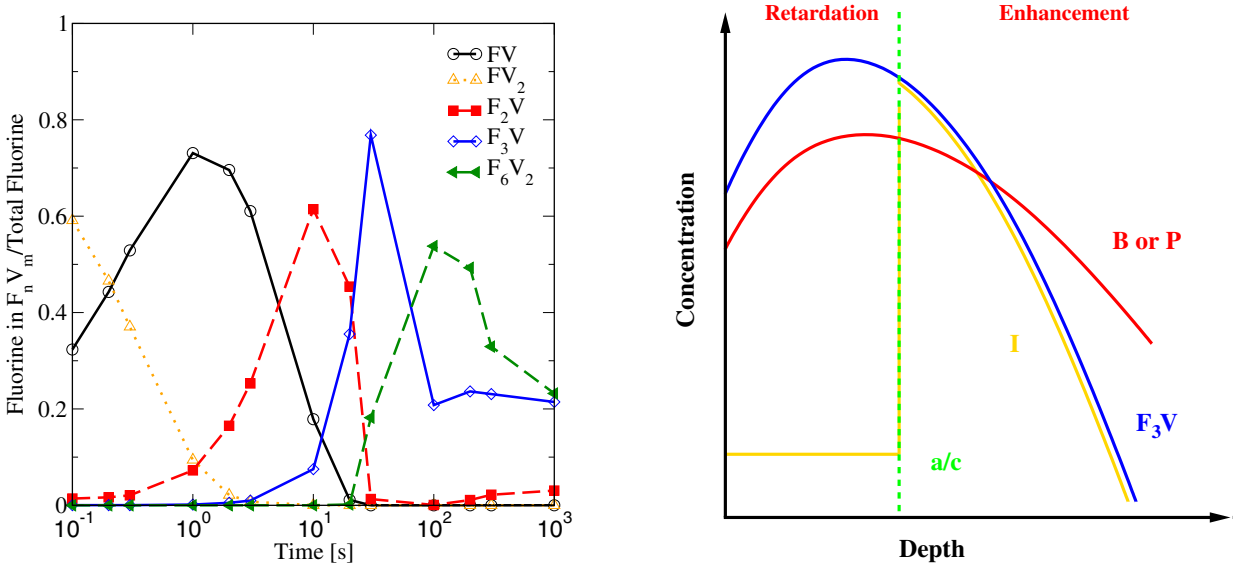

Figure 1: Left: Simulated fluorine dose versus time during a 30min anneal at 650°C after a 10^{13}cm^{-2} 30keV F^+ implant. The model used is described in detail in Ref. [7]. Only the most significant F_nV_m clusters are shown here. The time evolution can be split into two phases; phase 1: formation of F_3V and F_6V_2, phase 2: dissolution of F_3V and F_6V_2. Right: This diagram illustrates the mechanism by which F impacts B and P diffusion. The depth of the amorphous-crystalline interface (dashed green line) and the implant depth of fluorine are the key parameters. In the non-amorphized regions B and P diffusion get enhanced due to excess interstitials I, while in amorphized regions diffusion is retarded due to grown in F_3V.

Previously, a multi-cluster continuum model was developed that considered formation of various F_nV_m cluster configurations based on *ab-initio* calculations [7]. The model considered a large set of F_nV_m clusters and their associated reaction pathways successfully explained the anomalous fluorine diffusion behavior in silicon [7]. In this work, we analyze this model to derive a simpler form of the fluorine model.

Figure 1 (left) illustrates the time evolution of the dominant F_nV_m clusters using the multi-cluster model during a 30min anneal at 650°C under sub-amorphous conditions. This time evolution can be split into two phases: formation of F_3V and F_6V_2, and dissolution of F_3V and F_6V_2. Since the first phase is very brief (20s at 650°C, 0.5ms at 1000°C), we can focus only on the dissolution of the clusters. Since both dominant clusters have a 3:1 F:V ratio, we include only F_3V clusters. In the model, the complete F dose is implanted as F_3V (3 interstitial F atoms decorating a vacancy [7]). That effectively introduces +2/3 I for every F atom. Since we expect implanted F to be interstitial fluorine F_i (+1 I model), we correct by implanting the missing +1/3 I separately. This treatment is also applicable in the amorphous region, where we assume that F_nV_m clusters are grown in during the regrowth process since this minimizes the free energy of the regrown region. Figure 2 (left) shows the local equilibrium concentrations of different F_nV_m as a function of total F concentration at 650°C. For total F concentrations above 10^{14}cm^{-3} the dominant clusters are F_3V and F_6V_2. Since both clusters have the same F:V ratio, in the simplified model only F_3V is used. The

fluorine effects are modeled via a one cluster dissolution reaction:

$$F_3V + I \Leftrightarrow 3F_i \quad (1)$$

Figure 1 (right) illustrates the interaction mechanism of F on B and P via local point-defect concentration modifications. The diagram shows schematically F, dopant, and interstitial profiles after regrowth. In the amorphous region (left of a/c interface), vacancies (V) are grown in as F_3V clusters, which leads to TED reduction of B and P. In regions which are not amorphized, F enhances dopant diffusion due to the excess +1/3 I. This treatment enables the model to predict the fluorine effect on B and P in cases where the dopant concentration is divided by the amorphous-crystalline interface. The depth of the amorphous-crystalline interface and the implant depth of fluorine become the key parameters to understand the effect of fluorine on B and P.

RESULTS

The model introduced in the previous section was implemented and compared to experimental data for a range of conditions. Figure 2 shows the profiles of 20keV 3×10^{15}cm^{-2} F as-implanted and after a 1050°C spike anneal in the absence of other dopants. The implantation was performed through a 10nm screen oxide. The model predicts correctly the characteristic anomalous fluorine diffusion behavior. The SIMS data suggests the amorphous-crystalline (a/c) interface to be at 36nm, visible through the F accumulation at the end-of-range (EOR), whereas the simulation data indicates an a/c depth of 55nm. In all subsequent graphs the simulation value of the a/c depth is indicated for profile prediction. The trapping of F in the pre-amorphized region strongly supports the assumption of formation of F_nV_m clusters in the amorphized region during regrowth.

The impact of F on B and P is compared for two different experimental conditions: high energy/high dose implants (source/drain conditions) and high energy/low dose implants (halo conditions). Figure 3 (left and right) shows the effect of F on P diffusion. In the left graph (source/drain condition) an arsenic pre-amorphized sample was implanted with 4×10^{15}cm^{-2} P. The effect of F is investigated via 2×10^{15}cm^{-2} F implants at 10keV and 30keV and a 1050°C spike anneal. In all cases, most of the P dose is located within the pre-amorphized region. The a/c interface from MC simulations is at 55nm for no F and 10keV F implant. The P diffusion retardation effect due to co-implanted F is correctly predicted by the model (line with open circles). For the 30keV F implant, the a/c interface moves to 90nm. The model predicts an increased retardation effect due to the deeper pre-amorphized region, which is confirmed by the experimental data (line with filled squares). Under all conditions the simulation data matches the SIMS data well. F retards P diffusion since most of the P dose is initially located within the pre-amorphized region.

Figure 3 (right) shows SIMS data of a Sb/BF_2 pre-amorphized sample including a 40keV 9×10^{13}cm^{-2} P implant (halo condition). The effect of F is investigated via a 20keV 10^{15}cm^{-2} F implant followed by 950°C and 1050°C spike anneals. The a/c interface is located at 55nm. The SIMS data shows a retardation of the P diffusion in the presence of F. This behavior is matched well by the model. The retardation effect takes place primarly in the sub-amorphous region, but since the a/c interface is close to the tail of the P profile this is anticipated by

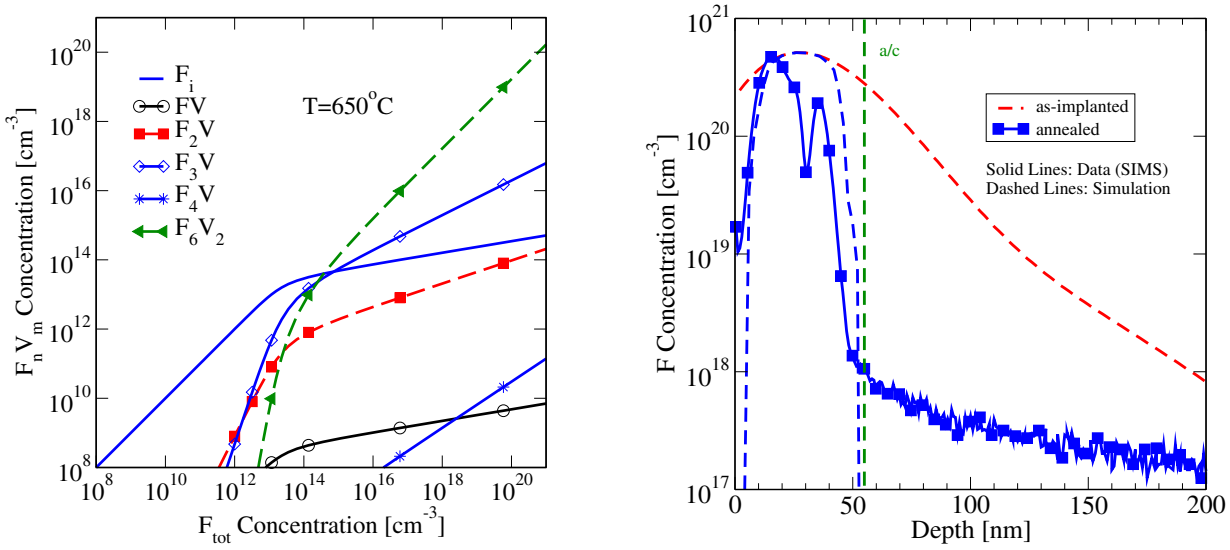

Figure 2: Left: F_nV_m concentration vs. total F concentration in local equilibrium at 650°C. Right: Measured and predicted concentration profiles of 20keV 3×10^{15}cm^{-2} F before and after a 1050°C spike anneal in the absence of other dopants.

the model. The experimental data as well as the simulation results show a shift in the peak location of the P profile due to coupling with the shallow B profile ($x_j \approx 30$nm). In the presence of F, the P peak movement toward the surface is retarded.

Figure 4 (left and right) shows B data under similar implant conditions to Fig. 3 for P. In the left graph a dose of 3×10^{15}cm^{-2} B is implanted (source/drain condition) and the effect of F is investigated via a 10keV 2×10^{15}cm^{-2} F implant and a 1050°C spike anneal. The a/c interface is located at 60nm. The B profile is slightly retarded in the presence of F as predicted by the simulation.

Figure 4 (right) shows a shallow As pre-amorphized sample including a 10keV 6×10^{13}cm^{-2} B implant (halo condition). The effect of F is investigated via a 10keV 10^{15}cm^{-2} F implant followed by 950°C and 1050°C spike anneals. The a/c interface is located at 28nm. The SIMS data shows an enhancement of the B diffusion in the tail region of the profile in the presence of F, which is matched well by the simulated data. Since there is only shallow pre-amorphization, this behavior is anticipated by the underlying model.

CONCLUSIONS

In summary, a simple model that incorporates the essential physics from *ab-initio* calculations was developed. This model predicts the effect of fluorine on boron and phosphorus diffusion under a range of experimental conditions. The behavior is predicted correctly in all cases, but there is a trend to overestimate the retardation effect seen in experimental data. This may be due to simulated a/c interface depths being deeper than the actual values as suggested by Fig. 2 (right).

This analysis predicts the F effect on B and P to be entirely due to interactions of F

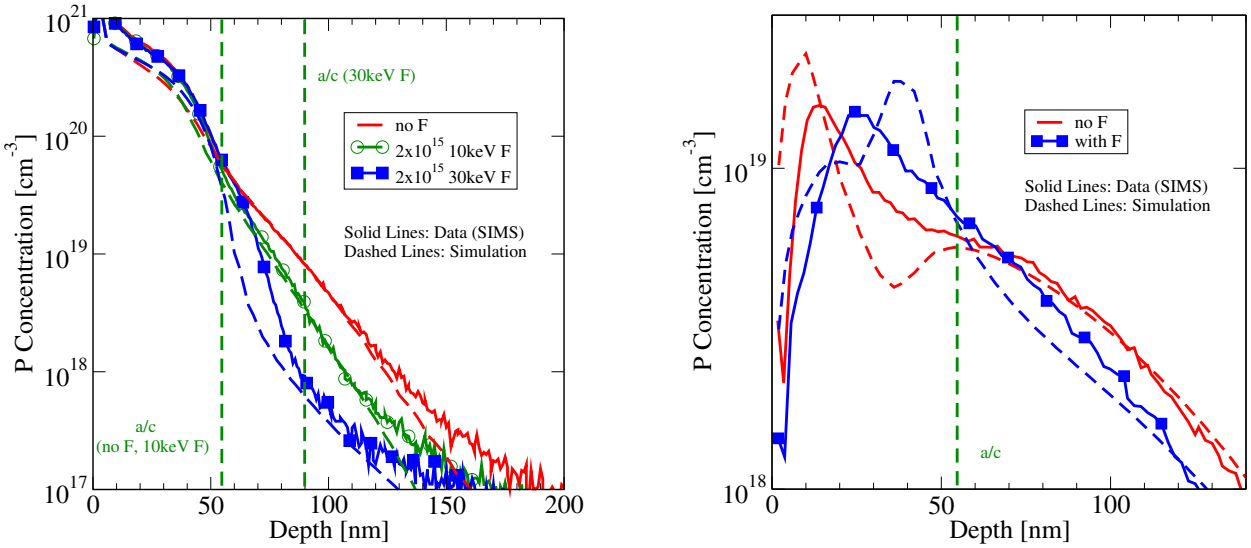

Figure 3: Left: Arsenic pre-amorphized sample with a 4×10^{15}cm^{-2} P implant. The effect of F is investigated via 2×10^{15}cm^{-2} F implants at 10keV and 30keV and a 1050°C spike anneal. Right: Sb/BF_2 pre-amorphized sample including a 40keV 9×10^{13}cm^{-2} P implant. The effect of F is investigated via a 20keV 10^{15}cm^{-2} F implant followed by 950°C and 1050°C spike anneals.

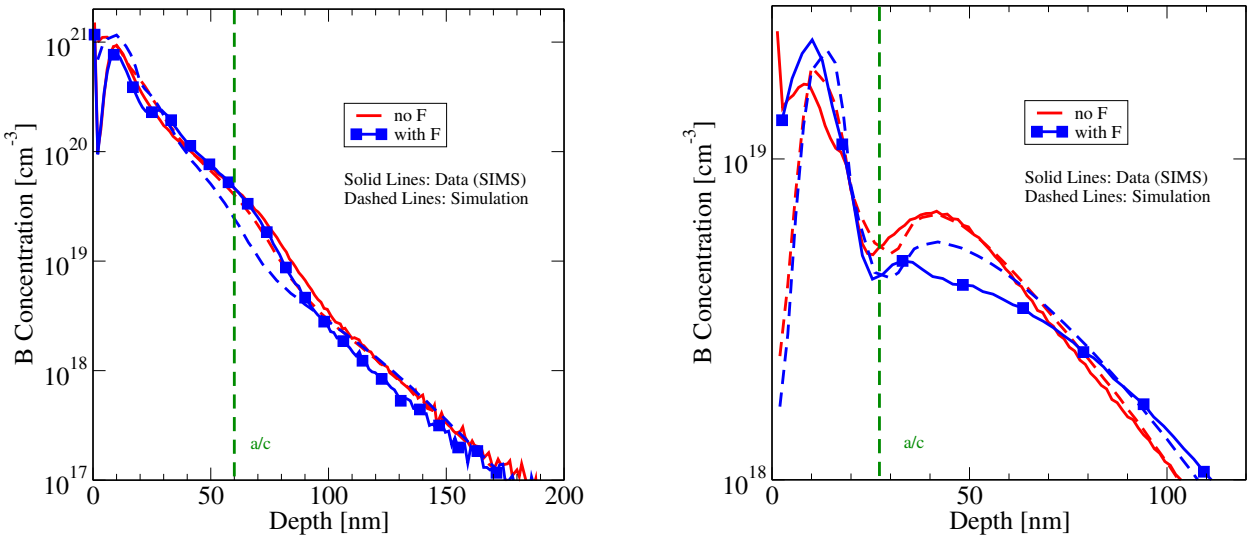

Figure 4: Left: A dose of 3×10^{15}cm^{-2} B is implanted and the effect of F is investigated via a 10keV 2×10^{15}cm^{-2} F implant and a 1050°C spike anneal. Right: Shallow arsenic pre-amorphized sample including a 10keV 6×10^{13}cm^{-2} B implant. The effect of F is investigated via a 10keV 10^{15}cm^{-2} F implant followed by 950°C and 1050°C spike anneals.

with point-defects. Fluorine alters the local point-defect concentration due to the formation and dissolution of energetically favored F_nV_m clusters and therefore indirectly impacts the

point-defect mediated diffusion behavior of B and P. The depth of the amorphous-crystalline interface and the implant depth of fluorine are the key parameters to understand the effects on dopant redistribution. Under sub-amorphizing conditions, B and P diffusion are enhanced, in contrast to amorphized regions where the model predicts retarded diffusion.

ACKNOWLEDGMENTS

This research was funded by the Semiconductor Research Corporation (SRC).

REFERENCES

[1] S.-P. Jeng, T.-P. Ma, R. Canteri, M. Anderle, and G.W. Rubloff, Appl. Phys. Lett. **61**, 1310 (1992).

[2] T.H. Huang and D.L. Kwong, Appl. Phys. Lett. **65**, 1829 (1994).

[3] J. Park and H. Hwang in *Si Front-End Processing: Physics and Technology of Dopant-Defect Interactions*, edited by H.-J. L. Gossmann, T.E. Haynes, M.E. Law, A.N. Larsen, and S. Odanaka, (Mater. Res. Soc. Symp. Proc. **568**, Warrendale, PA, 1999) pp. 71-75.

[4] D.F. Downey, J.W. Chow, E. Ishida, and K.S. Jones, Appl. Phys. Lett. **73**, 1263 (1998).

[5] L.S. Robertson, P.N. Warnes, K.S. Jones, S.K. Earles, M.E. Law, D.F. Downey, S. Falk, and J. Liu in *Si Front-End Processing: Physics and Technology of Dopant-Defect Interactions II*, edited by A. Agarwal, L. Pelaz, H-H. Vuong, P. Packan, M. Kase, (Mater. Res. Soc. Symp. Proc. **610**, Warrendale, PA, 2000) pp. B4.2.1-B4.2.6.

[6] H.W. Kennel et al., 2002. IEDM '02. Digest. International , 875, (2002).

[7] M. Diebel and S.T. Dunham in *Si Front-End Junction Formation Technologies*, edited by D.F. Downey, M.E. Law, A.P., Claverie, M.J. Rendon, (Mater. Res. Soc. Symp. Proc. **717**, Warrendale, PA, 2002) pp. C4.5.1-C4.5.6.

[8] M. Diebel and S.T. Dunham (paper in preparation).